6th European Conference on Computational Mechanics (ECCM 6)
7th European Conference on Computational Fluid Dynamics (ECFD 7)

11 – 15 June 2018, Glasgow, UK

HOT WIRE ANEMOMETRY AND NUMERICAL SIMULATION APPLIED TO THE INVESTIGATION OF THE TURBULENCE IN A GAP FLOW

Herbert A.M. Severino[1], Tiago de Melo[2] and Jhon N.V. Goulart[3]

Group of experimental and computational Mechanics - University of Brasilia
Gama, 72.405-610, Brazil
[1] herbert.ams@gmail.com. [2] tiago.melomec@gmail.com, [3] jvaz@unb.br.

Key words: Hot Wire Anemometry, SST Turbulence Model, Gap Flow, Large Vortices.

Abstract. Hot-wire anemometry and numerical simulation were employed to study the features of the turbulent flow and the large-scale structure formation in a closed compound channel. This work is aimed to characterize the structure of the turbulence in a rectangular channel containing a single rod bundle $D = 60\ mm$. The work was carried out numerical and experimentally. In the experimental campaign a single rod bundle, as long as $33.33\ D$, is placed in a rectangular channel. The rod is carefully located near the channel's top wall forming a narrow gap, $d = 0.10\ D$, between the rod and the wall, which connects two main channels. We run our experiments using single straight hot-wire probes in order to obtain the velocity fluctuations and the mean average fields of turbulence intensity and axial velocity as well. The experimental work was performed under three different Reynolds numbers, $Re_{Dh} = 26500, 52100$ and 86400, based on the bulk velocity, U_{bulk}, the hydraulic-diameter, D_h, and the kinematic viscosity, v of the fluid (air). As regards to the numerical computations k-ω-SST- model was applied to simulate the turbulent flow in a same geometry before experimentally studied. However, to safe computational resources we choose to apply translational periodicity between the channel's inlet and outlet and decrease the Reynolds number as well, to $Re_{Dh} = 8000$. To implement the periodicity we followed the steps suggested by [2] the computational domain reached $8\ D$. Through auto-correlation and *PSD* tools the main frequency and the Strouhal number were computed. The spectral analyses showed different values in terms of frequency, however, when the Strouhal number is computed, based on the bulk velocity U_{bulk}, the main frequency, f, and the rod's diameter, D, both results were found almost constant, $St = 0.16$, which is in fair agreement with experimental works from Guellouz and Tavoularis [9 and 10].

1 INTRODUCTION

Quasi-periodic oscillation in the narrow gap is one of the most striking feature found in compound channels, does not matter if it is open or closed. Large scale motions in rod bundles are known for approximately a half century at least [2]. [3], was one of the pioneers to study the influence of the macroscopic structure of the turbulent main flow in the mixing process in a compound channel. The author worked with a rod package arranged parallel to the flow in order to determine the convective coefficients of heat transfer in one of the bars. The most relevant conclusion was to show that in the vicinity of the subchannels the autocorrelation functions of the time series of velocity fluctuation were similar to damped

sinusoidal functions, thus suggesting the presence of large vortices crossing the narrow gap between the subchannels.

Then the frequency and amplitude of these oscillations for array of bare rods geometries and Reynolds number were the target of several authors. (e.g. [4]; [5]; [6]; [7] and [8]). Many studies have been developed experimentally ([9];[10] and [11]);. An appearance of these structures is observed even in laminar flow view in [12].

Guellouz and his co-work contributed with a characterization of large scale structures in a rectangular channel containing a cylindrical rod near the bottom wall [9 and 10]. The work was developed under Reynolds number 1.08×10^5 based on the hydraulic diameter, bulk velocity and air viscosity, time-average axial velocity. Reynolds stress and turbulent kinematic energy were also target of the investigation along with the dynamic of the flow, as well. So, the authors estimated the Strouhal number, the wavelength, the convective velocity and coefficient of friction in the rod wall. From the experimental measurements they concluded that the spanwise velocity component presented a strong periodicity suggestion that coherent structures dominated the gap vicinity.

Numerical work was, some time after, carried out by Chang and Tavoularis [13 and 14], in order to understand better the experimental results from Guellouz [9]. The authors performed numerical computations on the same cross-section with W/D-ratio = 1.10. To predict the dynamic behaviour Unsteady Reynolds Average Navier Stokes (URANS) was used along with different turbulence models and translational periodicity. The authors were able to identify the coherent structures using the criterion Q (which will be discussed below), but the mean values of velocity and the turbulent kinetic fields presented some discrepancy compared to the experimental results.

The work is aimed to study the structure of the turbulent flow in the narrow gap of a rectangular channel containing an eccentric cylinder near the top wall. By means of numeric technique and hot wire anemometry the mean average velocity fields and the dynamic of the flow was predicted. The dynamics of the large-scale structures, such as the main frequency, wavelength and the convection velocity were studied in detail, likely [15]. Numerical work was developed using the ANSYS® CFX package using the Unsteady Reynolds Averaged Navier-Stokes (URANS) and Shear Stress Transport- SST model to predict the turbulence. The Reynolds number, based on the bulk velocity, U_b, the hydraulic-diameter, D_h and the kinetic viscosity was $Re_{Dh} = 8000$. To minimize the computational cost, periodic boundary conditions in the streamwise direction were applied, reducing significantly the domain compared to the experimental work. The strategy computational is applied successful for several author e.g. [15, 17, 18, 19, 20, 21, 22, 23].

As regards the experimental work, this one was developed under three different Reynolds numbers, 26500, 52100 and 86400. Reynolds number was based on the same scales in both numerical and experimental works.

2 EXPERIMENTAL PROCEDURE

The experiments were conducted in a closed channel in steady state regime. Water at room temperature ($\approx 25°C$) was used as work fluid. The work fluid was driven by a centrifugal pump in closed loop. The compound channel is depicted in Fig. 1a and 1b with constant section $L = 193\ mm$, $H = 151\ mm$ and total length $L_{tc} = 4000\ mm$ ($L = 3.3\ D$, $H = 2.5D$,

$L_t = 54.8D$). The fluid reaches the test section, after passing through a diffuser and a set of honeycombs. The test section contains one single rod with external and internal diameter $D = 60\ mm$, and the length $L_{sc} = 2000\ mm$ ($L_{sc} = 33.3D$). The rod is far from upper channel wall by a distance W, which produces a dimensionless number W/D. In this work W/D-ratio 1.10 was tested for, $Re_{Dh} = 26500$ up to 86400.

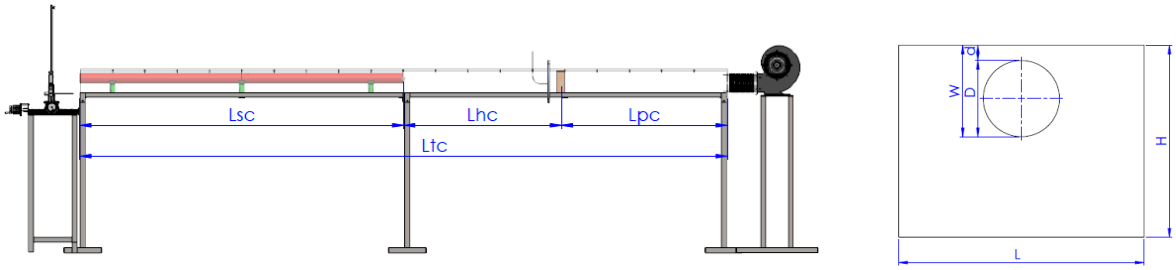

(a) (b)

Figure 1: Sketch of the flow facility. (a) Upper view; (b) Inside section view.

The hydraulic-diameter was computed through eq. 1

$$\mathrm{Re}_{Dh} = \frac{U_b D_h}{\nu} \rightarrow D_h = \frac{4A}{P} \tag{1}$$

A is area of the cross section and P is wet perimeter.

Experimental velocity fluctuations time-traces, in the streamwise direction, were gathered at 30 mm the channel's outlet upstream through a single hot wire probe. Data were sampled at 1 KHz for a time acquisition as long as 32,768 s. Data were also filtered by a low pass filter set at 300 Hz.

3 CFD METHODOLOGY

3.1 Geometry and flow conditions

As illustrated in Fig. 2a and 2b, the main computational geometry was the same as that one stressed in the previous experiment. It consisted of a single cylindrical rod with diameter D=60mm, inside a rectangular channel with width $L_x = 3.3D$ and $L_y = 2.5D$ similar experimental. The gap size of rod and upper wall of channel is $d = 6\ mm$, and therefore, yielding W/*D-ratio* $= 1.10$. However, the original length of the channel of $2000\ mm$ was significantly shortened to length $L_z = 480mm$ ($L_z = 8D$) adopted in this computation. This was made possible by employing periodic boundary conditions in the streamwise direction in combination with a fixed mass flow rate, $m = 1.95\ Kg/s$. At the walls the velocity was imposed null.

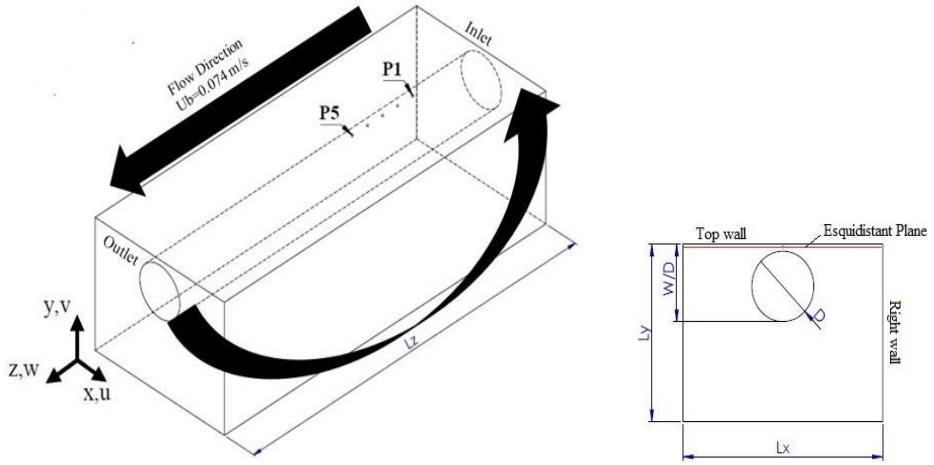

Figure 2: (a) Schematic view of compound; (b) Channel's cross-section and its dimensions.

3.2 Mesh Independence

In order to determine the length of the domain in the main direction mesh study independence was carried out. Different length domains were evaluated, *Lz = 360 mm*, *480 mm*, *720 mm* (*Lz/D = 6*, *8* and *12*). For the first one, *Lz/D = 6*, it was not possible to solve the mass balance in good accuracy as we expected. For the computational domains *8D* and *12D* there was no significant dynamic variation of the flow. So, we chose the smaller one, $L_z/D = 8$. All meshes were discretized with hexahedral volumes, by splitting up the computational domain into smaller ones. In the upper channel's wall and rod wall the mesh was refined to obtain a $y^+ < 1$. In the other walls of the cross section a refinement was applied yield $y^+ \approx 10$. In streamwise direction z^+ was chosen to be about 25. Fig. 3a shows the mesh used in a cross-section. It should be noticed the mesh refinement near the top wall and around the tube.

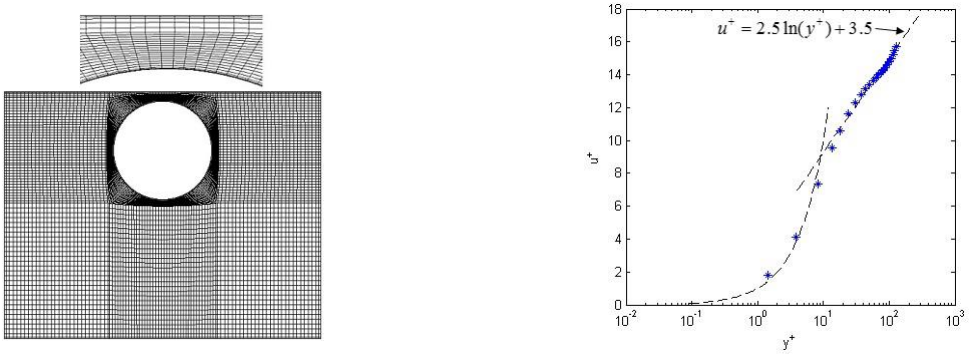

(a) (b)

Figure 3: (a) Mesh of the cross-section. (b) Law of the wall obtained at L_x/D=1, L_z/D=4, near the top wall.

The whole simulation was performed with a time step equivalent to *0.005 s*, with the Courant- Friedrichs- Lewy $CFL_{max} \approx 0.35$.

In Fig. 3b the good quality of the numerical simulation and the mesh can be observed. The velocity near the rod surface is plotted as a function of y^+. From the Fig. 3b we see that the mesh was able to describe in a good way the subviscous layer, that is required by $k-\omega$ - SST model. In addition, the classic wall function was practically recovered.

4 K-ω SST MODEL FORMULATION

The SST model was proposed by [24]. In this model, the formulation of the *k*–*ε* model is used far from the wall region and near the wall is applied *k*–*ω* model. The zonal formulation is based on blending functions, which ensure a proper selection of the *k*–*ε* and *k*–*ω* zones. The basic formulation of the incompressible continuity and Navier-Stokes equations are

$$\frac{\partial \overline{u_i}}{\partial x_i} = 0 \tag{2}$$

$$\rho\left(\frac{\partial \overline{u_i}}{\partial t} + \overline{u_j}\frac{\partial \overline{u_i}}{\partial x_j}\right) = -\frac{\partial \overline{p}}{\partial x_i} + \mu\frac{\partial^2 \overline{u_i}}{\partial x_j^2} + \frac{\partial \tau_{ij}}{\partial x_j} \tag{3}$$

The complete formulation of the SST model is given, with the limited number of modifications highlighted.

$$\frac{\partial(\rho k)}{\partial t} + \frac{\partial(\rho U_i k)}{\partial x_i} = P_k - \beta^*\rho k\omega + \frac{\partial}{\partial x_i}\left[\left(\mu + \frac{\mu_t}{\sigma_k}\right) + \frac{\partial k}{\partial x_i}\right] \tag{4}$$

$$\frac{\partial(\rho\omega)}{\partial t} + \frac{\partial(\rho U_i \omega)}{\partial x_i} = \alpha\rho S^2 - \beta\rho\omega^2 + \frac{\partial}{\partial x_i}\left[\left(\mu + \frac{\mu_t}{\sigma_\omega}\right)\frac{\partial \omega}{\partial x_i}\right] + 2(1-F_1)\rho\sigma_{\omega 2} + \frac{1}{\omega}\frac{\partial k}{\partial x_i}\frac{\partial \omega}{\partial x_i} \tag{5}$$

The turbulence eddy viscosity is defined as follows:

$$\nu_t = \frac{\alpha_1 k}{\max(\alpha_1\omega, (S_{ij}S_{ij})^{1/2}F_2)} \tag{6}$$

Where *S* is the invariant measure of the Strain Rate. The blending function is based on the distance to the nearest surface on the flow variables

$$F_1 = \tanh(\arg_1^4) \tag{7}$$

$$\arg_1 = \min\left[\max\left(\frac{\sqrt{k}}{\beta^*\omega}, \frac{500\nu}{y^2\omega}\right), \frac{4\rho\sigma_{\omega 2}k}{CD_{k\omega}y^2}\right] \tag{8}$$

with $CD_{k\omega}$ is defined for Eq. 9 and *y* is the distance to the nearest wall. F_1 is equal to zero away from the surface (*k* − *ε* model), and switches over to one inside the boundary layer (*k* − *ω* model).

$$CD_{k\omega} = \max\left(2\rho\sigma_{\omega 2}\frac{1}{\omega}\nabla k\nabla\omega, 1, 0.10^{-10}\right) \tag{9}$$

F_2 is a second blending function defined by:

$$F_2 = \tanh\left(\left[\max\left(\frac{2\sqrt{k}}{\beta^*\omega y}, \frac{500\nu}{y^2\omega}\right)\right]^2\right) \tag{10}$$

A production limit used in the SST model to prevent the rise of turbulence in stagnation regions:

$$P_k = \mu_t \frac{\partial U_i}{\partial x_j}\left(\frac{\partial U_i}{\partial x_j}+\frac{\partial U_j}{\partial x_i}\right) \rightarrow \tilde{P}_k = \max(P_k, 10\cdot\rho\beta^* k\omega) \tag{11}$$

All constants are computed by a blend from the corresponding constants of the k − ε model and k − ω model via $\alpha = \alpha_1 F_1 + \alpha_2(1-F_1)+...$ The constants for this model are $\beta^* = 0.09$, $\alpha_1 = 5/9$, $\beta_1 = 0.075$, $\sigma_{k1} = 0.85$, $\sigma_{\omega 1} = 1/2$, $\alpha_2 = 0.44$, $\beta_2 = 0.0828$, $\sigma_{\omega 2} = 0.856$, $\sigma_{k2} = 1$.

5 RESULTS AND DISCUSSION

5.1 Mean Averaged Quantities

In Fig. 4 the time-average isocontours of the streamwise velocity is showed along with the results published years ago by [9]. The data were gathered in the middle of the computational domain at $Lz/D = 4$, being stressed in dimensionless form by the bulk velocity, U_b. All quantities were averaged over a time $t = 16T_c$, where T_c is the convective time, $T_c = L_z/U_b$. In general form $k-\omega$ SST was able to capture some remarkable features of the mass flow rate distribution in this kind of compound channel. Numerical methodology was able to predict the very well pronounced bulging of the isolines towards the edges arisen from the secondary flows according to [25]. In a qualitative way both velocity maps are in good agreement despite the Reynolds number difference. The maximum axial velocity is W/U_b was found about 1.20 taking place at the main subchannel. At the same location Guellouz and Tavoularis found $W/U_b = 1.17$, (Fig. 4 (a) and (c)). However, the mass distribution has found its strongest discrepancy near to the narrow gap. The zone at the gap was magnified, Fig. 4 (b), to provide a better comparison with Guellouz's experiment. There we can see quite similar isoline patterns in both works, however, our values seemingly are scaled by a factor of *0.5* in comparison to the experimental work. Such discrepancy may be attributed to Reynolds difference between numerical and experimental works, *8000* and *108000*, respectively.

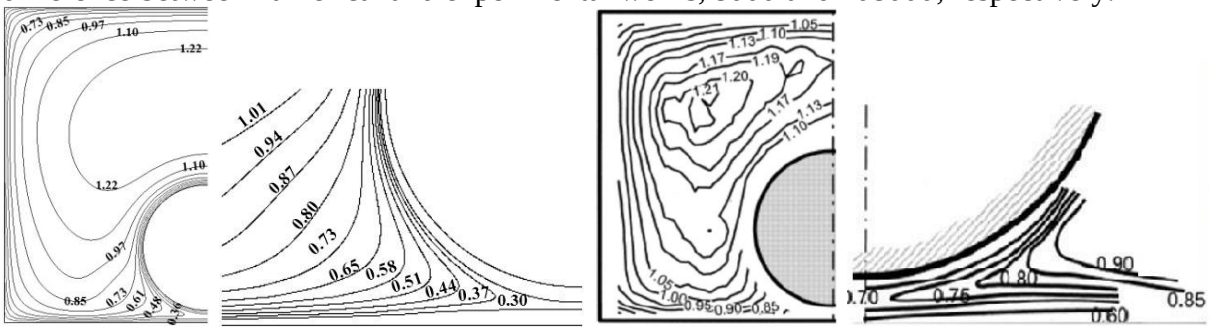

(a) (b) (c) (d)

Figure 4: Isolines of streamwise velocity components. (a) and (b) present work. (c) and (d) work from Guellouz and Tavoularis (2000a).

5.2 Kinetic Energy Distribution

In the same way Fig. 5 shows the isolines patterns the kinetic energy inside the channel. The data were gathered at the same location, $L_z/D = 2$, and averaged over the same aforementioned time. Data are also stressed in dimensionless form $k^* = k/U_b^2$. Although there is a remarkable difference between both Reynolds number, the numerical and experimental results are in good agreement, mainly far from the gap region. Near the lateral wall the numerical code predicted k^* about *0.012*, whereas the experimental map shows *0.01*. Again,

the difference really matters when the turbulent quantities are analyzed at gap vicinity. The prediction of k^* at this region was found lowered in one order when compared to the experimental work. It is worth to mention that the Reynolds number for numerical computation is also one order lower than experimental work carried out by [9], so such difference may attributed by the Reynolds number.

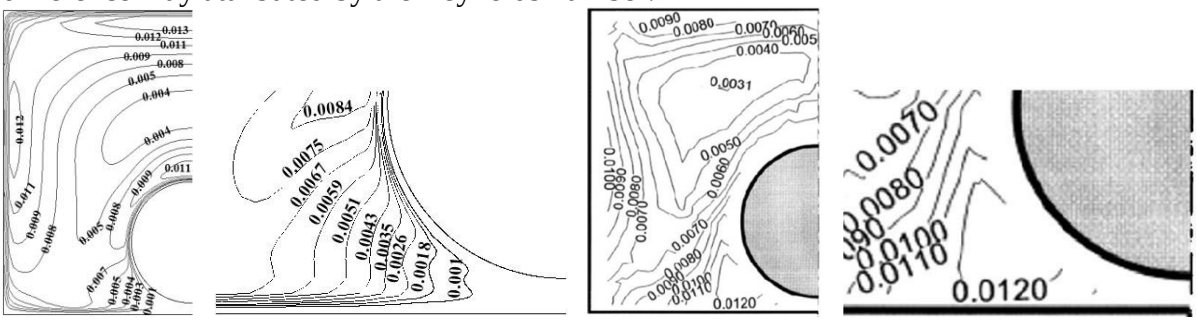

Figure 5: Isocontours of average turbulent kinetic energy. (a) and (b) present simulation. (c) and (d) experimental work from Guellouz and Tavoularis (2000a).

5.3 Coherent structures characterization

One of the most striking characteristic of the turbulent flow in compound channels are the quasi-periodic flow patterns of the velocity time-traces. The periodicity of the flow field suggests the presence of large scale coherent structures in the flow. Such velocity pattern (and therefore coherent structures) is responsible for heat, mass and momentum exchanging between adjacent sub channels throughout the narrow gap. Such behavior implies, for instance, in the convective heat coefficient enhancement as well as the local mixing rates. Quasi-periodic flow was also found even in laminar flow-state with Reynolds number ranging from *900* up to *1800*, [26]. Fig. 6 shows the streamwise velocity time-traces. The results are made non-dimensional by the bulk velocity, U_b. The velocity time-traces were gathered at the middle gap, between the rod and bottom wall, at the position L_x/D = 6, for numerical work and 30 mm upstream of the channel's outlet. For experimental work hot wire anemometry technique was employed.

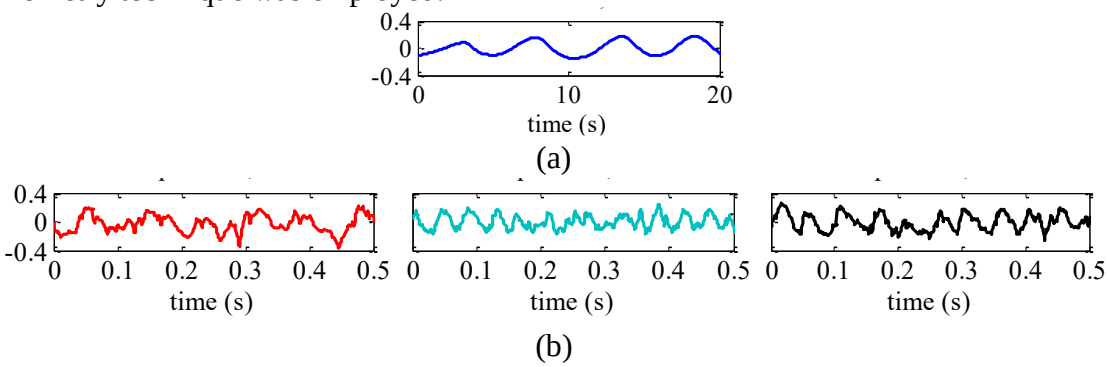

Figure 6: Numerical and experimental axial velocity fluctuations time-traces. a) Numerical Re_{Dh} = *8000.* b) Hot wire probe measurement, Re_{Dh} = *26500, 52100* and *86400.*

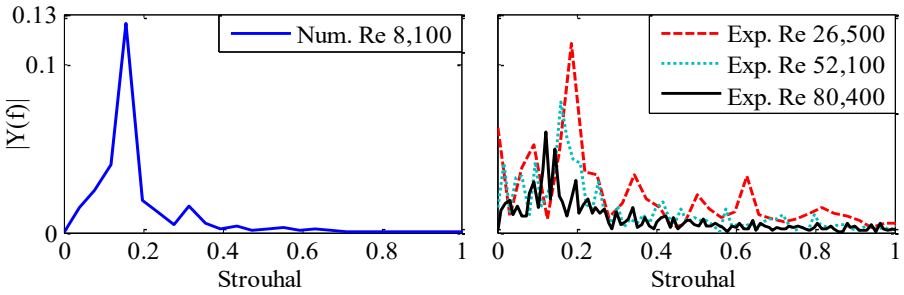

Figure 7: FFT for streamwise velocity fluctuations component.

First of all, quase-periodic velocity time traces were found as in our computations as in the experimental measurements, Fig. 6 (a) and (b). Furthermore, the computations was able to predict the excursion the velocity fluctuation as well, that was found to departure from w/U_b = -0.40 up to 0.40, regardless the Reynolds number. Fast Fourier Transform was applied to each velocity fluctuation time-trace, in order to calculate the fundamental frequency of the time-serie. In the computational result that one was found $f = 0.182$ *Hz*. However, higher frequencies were found in the experimental campaign as the Reynolds number increases, Fig.6 (b). Such fact was already expected, since the bulk velocity has increased as well. In order to compare the dynamic of the large motion for both experimental and numerical simulation, we make the frequency dimensionless as proposed by Guellouz and his co-worker [9]. The Strouhal number is then written,

$$St = \frac{fD}{U_b} \tag{12}$$

where, f is the main frequency attributed to the large periodic motions, *Hz*, D is rod's diameter, and U_b, is the bulk velocity. At that time the experimental results for the same geometry and W/D – ratio 1.10 produced $St = 0.17$, according to the authors. Based on the same scales used by the authors we calculated the Strouhal number of the numerical results, that was found $St = 0.15$. Such value was quite similar to that one published years ago by the authors, despite the Reynolds number difference. It is important to remind the reader that the Reynolds number for experimental work is *108000*, and, therefore, one order greater than ours, *8000*. This result also suggests that the dynamic of the flow is slightly affected by the Reynolds number which, in some degree, corroborates with Melo's work [30]. The experimental work published recently by Melo showed that the Strouhal number value is much more affected by the geometry of the compound channel than the Reynolds number itself. The gap width and the channel's length were found to play a very important role in the large vortices appearance and the spectral detection in the time-trace velocities as well.

We furthered our computational analysis by estimating the convective velocity, U_c and the wavelength number, λ, of the large vortices. Both characteristics were estimated through the velocity time series. The convective velocity is the velocity which the large vortices travel downstream the flow. It can be computed from the Eq. 13.

$$U_c = \lambda f \tag{13}$$

In eq. 13, f is the fundamental frequency of the large vortices and λ is the average space between two consecutive vortices that rotate in same direction.

The convective velocity was then calculated and is presented as a function of bulk velocity

yielding $U_c/U_b = 0.51$. Such value is lower than showed in the experimental work from Guellouz in 2000. According to the authors it should be about 0.78. However, the reader must take into account that the Reynolds number of the experimental work is one order greater than the present work and any direct comparison should be carefully evaluated. Furthermore, the dynamic characterization of the turbulent flow in this kind of geometry still needs reliable values for such Reynolds number range.

From the computed Strouhal number, *St*, and the convective velocity, *Uc*, the wavelength could also be determined. In the present work the numerical code predicted $\lambda/D = 3.6$. This number is slighted lower than published by Guellouz in 2000 whose experimental work showed $\lambda/D = 4.2$.

6 CONCLUSION

A numerical and experimental study was carried out to investigate the structure of the turbulence in a channel containing a single -rod. The rod was apart from the channel's top wall by a distance 6 *mm*, that yields *W/D – ratio 1.10*. Numerical computations were performed by using commercial code. The turbulence model was set to be $k-\omega$ SST for a Reynolds number *8000*. The numerical data were compared, as much as possible, with the results released by [9], who carried out an experimental work on the same topic and using similar geometry. Hot-wire probes were also employed to captures the velocity fluctuations time-traces in order to know the dynamic of the flow. So, three different Reynolds, numbers were investigated by varying the bulk velocity of flow in the experimental campaign. The Reynolds number was set from *26500* up to *86400*.

Mean average quantities were predicted by $k-\omega$ SST satisfactorily. Numerical results on mean axial velocity and turbulent kinetic energy were found in good agreement in comparison with experimental data from [9], despite de Reynolds number difference. However, some discrepancy could be observed. The strongest difference between both results was concentrated at the gap region. At that region both mean axial velocity and the turbulent kinetic energy were found lower than the experimental work from Guellouz. As regards the last one, this was predicted $k^*=0.001$ as the experimental work showed $k^*=0.012$. On the other hand, good predictions were achieved for the dynamic characteristics of the turbulent flow in the narrow gap.

The code was also able to predict, in very fair agreement, the wavelength, λ and the dimensionless convective velocity, U_c/U_b. Such values were compared to the experimental results released years ago by Guellouz [9], despite the Reynolds number difference. Among these three characteristics the worst case was the predicted convection velocity that was found $U_c/U_b = 0.51$ in our numerical simulation.

As regards to experimental campaign velocity fluctuation time-traces in streamwise directions were acquired with hot-wire probes. Regardless the Reynolds number and the way that the data were gathered every time-trace presented quase-periodic flow. The fundamental frequency was found to increase with the bulk velocity increase. However, when the main frequency was made dimensionless, through the Strouhal number, this one was found to collapse in Strouhal 0.15. Such number is slightly lower that one predicted years ago by Guellouz and Tavoularis [9] in their experimental work under a Reynolds number 108000. Furthermore, this fact also showed us that the Reynolds number seems to produce a little

effect in the in the dynamic behavior of the turbulent flow.

7 ACKNOWLEDGEMENTS

The authors would like to acknowledge the financial support provided by Fundação de Apoio a Pesquisa do Distrito Federal- FAP/DF.

REFERENCES

[1] Goulart, J.V.N., 2009. *Análise experimental de escoamentos cisalhantes em canais compostos fechados*. Ph.D. thesis, University Federal of Rio Grande do Sul, Brazil.

[2] Chang, D. and Tavoularis, S., 2012. "Identification of coherent structures in axial flow in a rectangular channel containing a rod". *Nuclear Engineering and Design*, Vol. 243, pp. 176–199.

[3] Rowe, D.S., Johnson, B.M. and Knudsen, J.G., 1974. "Implications Concerning Rod Bundle Crossflow Mixing Based on Measurements of Turbulent Flow Structure". *Int J Heat Mass Transfer*, Vol. 17, pp. 407–419.

[4] Hooper, J.D. and Rehme, K., 1984. "Large-scale structural effects in developed trubulent flow through closely-spaced rod arrays." *Journal Fluid Mech.*, Vol. 145, pp. 305 – 337.

[5] Möller, S.V., 1992. "Single-phase turbulent mixing in rod bundles". *Exp. Thermal and Fluid Science*, pp. 26–33.

[6] Wu, X. and Trupp, A.C., 1993. "Experimental study on the unusual turbulence intensity distributions in rod-to-wall gap regions". *Exp. Thermal Fluid Sci*, Vol. 6, pp. 360 – 370.

[7] Wu, X. and Trupp, A.C., 1994. "Spectral measurements and mixing correlation in simulated rod bundle subchannels." *Int.J.Heat Mass Transfer*, Vol. 37, pp. 1277 – 1281.

[8] Krauss, T. and Meyer, L., 1998. "Experimental investigation of turbulent transport of momemtum and enerfy in a heated rod bundle". *Nuclear Eng. Des.*, Vol. 180, pp. 185 – 206.

[9] Guellouz, M.S. and Tavoularis, S., 2000a. "The structure of the turbulent flow in a rectangular channel conteining a single rod-Part 1: Reynolds-Average measurements". *Exp Thermal and Fluid Science*, Vol. 23, pp. 59–73.

[10] Guellouz, M.S. and Tavoularis, S., 2000b. "The structure of the turbulent flow in a rectangular channel conteining a single rod-Part 2: phase-averaged measurements." *Exp Thermal and Fluid Science*, Vol. 23, pp. 75–91.

[11] Choueiri, G.H. and Tavoularis, S., 2014. "Experimental investigation o flow development and gap vortex street in an eccentric annular channel. Part 1. Overview of the flow structure". *J. Fluid Mech*, Vol. 752, pp. 521–542.

[12] Gosset, A. and Tavoularis, S., 2006. "Laminar flow instability in a rectangular channel with a cylindrical core." *Phys. Fluids*, Vol. 18, p. 044108.

[13] Chang, D. and Tavoularis, S., 2004. "Numerical simulation of developing flow and vortex street in a rectangular channel with a cylindrical core".

[14] Chang, D. and Tavoularis, S., 2005. "Unsteady numerical simulations of turbulence and coeherent structures in axial flow near a narrow gap". *Journal Fluids Engineering*, Vol. 127, pp. 458–466.

[15] Goulart, J., Wissink, J.G. and Wrobel, L.C., 2016. "Numerical simulation of turbulent

flow in a channel containing a small slot". *Inter Journal of heat and fluid flow*, Vol. 61, pp. 343–354.

[16] Meyer, L. and Rehme, K., 1994. "Large-scale turbulence phenomena in compound rectangular channels". *Exp. Thermal Fluid Sci*, Vol. 8, pp. 286–304.

[17] Merzari, E., Ninokata, H. and Baglietto, E., 2008. "Numerical simulation of flows in tight-lattice fuel bundles". *Nuclear Engineering*, Vol. 238, pp. 1703–1719.

[18] Duan, Y. and He, S., 2017. "Large eddy simulation of a buoyancy-aided flow in a non-uniform channel-Buoyancy effects on large flow structures". *Nuclear Engineering and Design*, Vol. 312, pp. 191–204.

[19] Gurunath, S.K., 2012. *Numerical Investigation of Coherent Structures in Axial Flow in Single Rod-Channel Geometry*. Master's thesis, Delft University of Technology, The Netherlands.

[20] Ferrari, J.M., Severino, H. and Goulart, J., 2016. "Determinação numérica da perda de carga e fator de atrito em canais compostos". In *Congresso Nacional de Engenharia Mecânica - CONEM2016*. Fortaleza, Brazil.

[21] Home, D., Arvanitis, G. and abd M S Hamed, M.F.L., 2009. "Simulation of flow pulsation in a twin rectangular subchannel geometry using unsteady reynolds averaged navier-stokes modelling". *Nuclear Engeenering Design*, Vol. 239, pp. 2964–2980.

[22] Home, D. and Ligtstone, M.F., 2014. "Numerical investigation of quasi-periodic flow and vortexstructure in a twin rectangular shbchannel geometry using deched eddy simulation". *Nuclear Engeenering Design*, Vol. 270, pp. 1–20.

[23] Derksen, J.J., 2010. "Simulation of lateral mixing in cross-channel flow". *Computer and Fluids*, Vol. 39, pp. 1058–1069.

[24] Menter, F.R., 1994. "Simulation of lateral mixing in cross-channel flow". *AIAA Journal*, Vol. 32, pp. 1598–1605.

[25] Meyer, L., 2010. "From discovery to recognition of periodic large scale vortices in rod bundles as source of natural mixing between subchannels âA˜T a review".˘ *Nuclear Engineering and Design*, Vol. 240, pp. 1575 – 1588. ISSN 0029-5493.

[26] Ferrari, J.M.S. and Goulart, J.N.V., 2015. "Simulação numérica do escoamento laminar em um canal complexo". *Revista Interdisciplinar de pesquisa em engenharia*, Vol. 1.

[27] Meyer, L. and Rehme, K., 1995. "Periodic vortices in flow though channels with longitudinal slots or fins". In *10th Symposium on Turbulent Shear Flows*. The Pennsylvania State University Park August 14-16.

[28] Goulart, J.N.V., Anflor, C.T.M. and Möller, S.V., 2013. "Static and dynamic characteristics of turbulent flow in a closed compound channel." *Rev. Fac. Ing. Univ. Antioquia*, Vol. 68, pp. 124–135.

[29] Souza, S.I.S., Cestaro, H.A.M. and Goulart, J.N.V., 2014. "Numerical investigation of heat transfer in a turbulent flow in channels with gap". *Eng. Térmica*, Vol. 13, pp. 96–103.

[30] Melo, T., Goulart, J., Anflor, C.T. and Santos, E., 2017. "Experimental investigation of the velocity time-traces of the turbulent flow in a rectangular channel with a lateral slot." *European Journal of Mechanics B/Fluids*, Vol. 62, pp. 130–138.